Performance of RAKE Reception for Ultra Wideband Signals in a Lognormal-fading Channel

J. Zhang, R. A. Kennedy, T. D. Abhayapala
Department of Telecommunications Engineering, RSISE
Australian National University, Canberra ACT 0200, Australia
Email: jian@syseng.anu.edu.au

***Abstract*— RAKE reception for Ultra Wideband is crucial as the radiated power is restricted to be very low and there exist many resolvable multipath components. In this paper, the effectiveness of RAKE reception is investigated analytically. First, the conditions under which the interference in the RAKE fingers can be ignored are discussed. Then a method is introduced to derive the explicit expression of RAKE performance for the various combining methods for a lognormal fading channel. Numerical results show that RAKE reception can greatly improve the performance, and equal gain combining has comparable performance with maximal ratio combining.**

I. Introduction

In the last few years, there has been a rapidly growing interest in Ultra Wideband (UWB) systems [1]–[4]. Combined with spread spectrum techniques, especially time-hopping (TH), ultra narrow pulses ($<$ 1ns) are modulated to convey information in UWB. To avoid interference against existing wireless systems, the radiation power is restricted to be very low. As RAKE reception [5] can collect multipath signals, and there exist many resolvable multipath components in UWB channels, a RAKE receiver could potentially be very helpful to UWB. But is it applicable and effective?

A RAKE receiver takes advantage of the ideal autocorrelation performance of spread spectrum codes to eliminate the interchip interference (ICI). So the finger spacing is generally assumed to be equal to the chip width according to the sampling theory. In the TH-UWB case, it is impractical to make a similar assumption due to the complex propagation phenomenon and the fact that the TH chip width is not necessarily the reciprocal of signal's bandwidth. This results in a group of random time-delays in a channel model. For such a model, without the careful design of TH-codes, the ICI will become significant and deteriorate the performance of RAKE. The conditions in which RAKE can work effectively in UWB systems will be discussed in section II-B.

Previous methods to evaluate the performance of RAKE receiver for UWB are constrained to the experimental ones [1], [6] due to the absence of widely accepted fading channel models, especially the amplitude distribution, which is critical to performance analysis. Empirical distribution [2] of the amplitude fading markedly differs from Rayleigh fading. This is possibly because UWB signals have high resolution and only a small number of multipath components fall within an interval of delay resolution. In contrast, Rayleigh fading is justified directly from the complex Gaussian assumption based on the Central Limit Theorem which requires large numbers of independent random variables. From the latest results generated by IEEE802.15sg3 [2], the lognormal distribution is recommended to best fit the measured amplitude fading in a UWB multipath channel. So a time-delayed line (TDL) model with lognormal-distributed amplitude is adopted in this paper.

Generally, performance evaluation of diversity reception is hardly tractable due to the complexity of the statistics. A strategy is suggested in section III to simplify this process so that explicit expressions of performance can be readily obtained for the various combining methods such as equal gain combining (EGC) and maximum ratio combining (MRC). Performance of RAKE reception is exemplified in terms of average combined SNR and average symbol error probability in section IV.

II. System Description

A. Channel Model

In [2], clusters and rays are used to account for the cluster phenomena in UWB propagations and double series of parameters are used accordingly. This model presents difficulties for evaluating RAKE performance analytically due to the use of random poisson process to simulate the arrival of rays and clusters and the resulted indeterminate mean power distribution of every path. To make analysis tractable, we simplify it to a TDL model which can be represented by the impulse response

$$h(t) = \sum_{\ell=1}^{L} a_\ell \delta(t - \tau_\ell) + n(t), \tag{1}$$

where $n(t)$ is AWGN with zero mean and variance σ_0^2, τ_ℓ is the multipath delay, the fading amplitude a_ℓ is real and its absolute value is lognormal distributed. When $20\log_{10}|a_\ell|$ is Gaussian distributed with mean u_ℓ and variance σ, the probability density function (pdf) of $|a_\ell|$ is

$$p(|a_\ell|) = \frac{20}{\ln(10)\sqrt{2\pi}\sigma|a_\ell|}\exp\Big(-\frac{(20\log_{10}|a_\ell| - u_\ell)^2}{2\sigma^2}\Big), \tag{2}$$

where $|\cdot|$ stands for absolute value. According to [2], σ is fixed and u_ℓ varies with ℓ. This distribution is denoted by

$|a_\ell| : \Lambda(u_\ell, \sigma^2)$ where Λ stands for lognormal distribution. The first and second moments of $|a_\ell|$ are given by

$$\mathrm{E}[|a_\ell|] = \exp(\ln(10)/20\ u_\ell + (\ln 10)^2/800\ \sigma^2), \quad (3)$$
$$\mathrm{E}[a_\ell^2] = \exp(\ln(10)/10\ u_\ell + (\ln 10)^2/200\ \sigma^2). \quad (4)$$

As we will see in III-A, the sum of two independent lognormal variables can be well approximated by another lognormal variable. This assures that the cluster-plus-ray model proposed in [2] can be well approximated by the model suggested here even when overlapping of rays in different cluster happening. The remained problem here is how to model the mean power of a_ℓ. Two methods are considered. The first one, considering a general single exponential decay, is widely used in the literature. But it does not reflect the dual exponential fading model in [2] well. This distribution can be expressed as

$$\mathrm{E}[a_\ell^2] = \varepsilon_0 \exp(-\tau_\ell/\Gamma), \quad (5)$$

where ε_0 is the mean energy of the first arriving path ($\tau_1 = 0$), Γ is the path decay factor. Then u_ℓ can be expressed as

$$u_\ell = 10/\ln(10)(\ln \varepsilon_0 - \tau_\ell/\Gamma) - \ln(10)/20\sigma^2. \quad (6)$$

The second one, specific to the model in [2], uses the mean power from the experimental data generated in [2] directly.

B. Conditions for Clean RAKE Output

A key condition in which a conventional RAKE works effectively is when ICI and intersymbol interference (ISI) can be ignored. Ideal autocorrelation performance of spread spectrum (SS) codes is always assumed and utilized to eliminate the ICI. Note that ISI can not be reduced in this way in most existing SS systems such as the widely used DS-CDMA. It is because the orthogonality of SS codes' autocorrelation could be destroyed by ISI unless the excess multipath delay is far smaller than the length of SS codes.

For TH-UWB, if the maximum multipath delay is as small as the frame period, ICI can be constrained to a small degree through deliberate adjustment of time-related system parameters due to the low duty cycle of UWB signals. This rarely happens in high-speed applications. In most cases, ideal autocorrelation and crosscorrelation of TH codes are required to reduce ICI.

There is little published work on TH codes to date. Two papers [3], [4], referring to the design of FH codes, discuss the method based on permutation sequences. It is indicated that the autocorrelation of TH codes is some kind of *coincidence* autocorrelation and equal to the number of overlapped positions [3], [4] (we restrict ourselves to the case of pure TH codes where no amplitude information of codes is utilized). It is emphasized that the maximum autocorrelation is highly related to the relationship between the chip numbers in a frame (N_c) and the period of TH codes (N_s, which is also the number of pulses used to represent a symbol normally). Only when N_c is not much smaller than N_s, TH codes can have desirable autocorrelation property. On the contrary, when $N_s \gg N_c$, designing TH codes with good autocorrelation is hardly possible.

For TH-UWB, ideal autocorrelation is not the only necessary condition to ensure ICI to be eliminated, modulation methods also determine the effect of cancelling ICI - a factor often ignored without justification. Poorly chosen modulations will cause similar decision variables to be generated by desired symbols and non-desired modulated symbols due to the correlation operation with multipath components. When the time jitter caused by modulations is smaller than the pulse width, this interference can be eliminated totally. This is based on the fact that the multipath resolution is generally larger than the width of pulse. The ordinary modulations combined with TH are M-ary PPM, antipodal (bipolar) modulation, amplitude modulation and variations of them. Among them, Orthogonal PPM will lead to large decision error because of the potential ICI among modulated symbols. So it is not applicable to TH-UWB without further design considerations. For overlapped PPM, the optimal modulation parameter is smaller than the width of a pulse since the values of the pulse's autocorrelation could be negative [7]. The other modulation methods cause little time jitter.

So in a system with TH codes having ideal autocorrelation and an adequate modulation method, ICI can be reduced to a negligible order. At the same time, ISI can also be reduced as long as the excess multipath delay is smaller than several symbol periods. This benefits from the property of low duty cycle and *coincidence* autocorrelation. Furthermore, in amplitude modulated systems especially those with bipolar modulation, the interference from ISI plus ICI can be smaller than that from the pure ICI due to cancellation between antipodal signals. In a RAKE receiver with J fingers, when ICI and ISI are ignorable, we could get a "clean" RAKE output and obtain the well-known expressions for instantaneous signal-to-noise ratio (i-SNR)

$$\gamma_s = \rho \frac{E_s}{\sigma_0^2} \frac{(\sum_{j=1}^{J} a_j g_j)^2}{\sum_{j=1}^{J} g_j^2}, \quad (7)$$

where g_j are the weights of RAKE fingers and depend on combining methods, ρ is the normalized correlation of a single pulse and a template signal in a frame period (and depends on the modulation method), E_s is the symbol energy of a transmitted signal and E_s/σ_0^2 can be regarded as the symbol SNR of the transmitted signal.

An application of the Cauchy inequality,

$$(\sum_{j=1}^{J} a_j g_j)^2 \leq \sum_{j=1}^{J} a_j^2 \sum_{j=1}^{J} g_j^2, \quad (8)$$

which has equality only when $g_j = a_j$, leads to the well-known maximal ratio combining (MRC) and the i-SNR becomes

$$\gamma_{s,\mathrm{MRC}} = \rho \frac{E_s}{\sigma_0^2} \sum_{j=1}^{J} a_j^2. \quad (9)$$

Supposing that the receiver knows the polarity of multipath components and combine all fingers' signals using $g_j = 1 \cdot$

$\text{sgn}(a_j)$, where $\text{sgn}(a_j)$ is the function of getting the sign of a_j. We call this equal gain combining (EGC) and the i-SNR becomes

$$\gamma_{s,\text{EGC}} = \rho \frac{E_s}{\sigma_0^2} (\sum_{j=1}^{J} |a_j|)^2 / J. \tag{10}$$

Under the assumption of independence between RAKE fingers, the statistical characteristics of i-SNR can be derived directly now. But for more general performance criteria, such as symbol error probability (SEP), derivation will involve joint probabilities and J-fold integrations and have high computational complexity if treated in a general way [8]. Fortunately, for the lognormal distribution in UWB applications, there are simplifications that make this tractable as discussed next in section III-A.

III. Performance Analysis

A. Distribution of the Sum of Lognormal Variables

We represent the instantaneous SNR γ_s as the product of a scalar λ and a random variable α, $\gamma_s = \lambda\alpha$. Then $\alpha = (\sum_{j=1}^{J} |a_j|)^2$ for EGC and $\alpha = \sum_{j=1}^{J} a_j^2$ for MRC.

The basic idea here is to find the pdf of α and substitute the joint pdf involved in performance analysis. There is a general agreement that a sum of independent lognormal random variables can be well approximated by another lognormal random variable when the spread of σ in (2) is not too wide (<30dB in our case[1]) [9]–[11]. Moreover, this approximation is also applicable to the sum of correlated lognormal variables. So the distribution of α can be treated as lognormal and represented as $\alpha : \Lambda(u_\alpha, \sigma_\alpha^2)$. Different approaches to find the parameters of the resultant lognormal distribution have been proposed. The Wilkinson approximation (WA) and Schwarz and Yeh approximation (SYA) [10] are most common. The former, which is simpler, first computes the mean and variance of the sum applying the general statistical formulae, and then calculates u_α, σ_α and the pdf through (3)-(4) implicitly; the latter starts in an inverse order, that is, find the mean and variance of the variable $Z = \ln(e^{Y_1} + e^{Y_2})$ where Y_1 and Y_2 are two Gaussian variables. The obtained mean and variance of Z are u_α and σ_α, respectively if $\alpha = e^Z$ where Z is a Gaussian variable implicitly. It is generally believed that SYA can give better accuracy. A simpler and more accurate algorithm for SYA is given in [11].

In our opinion, the substance of the arguments is how to find a distribution to best fit the one that already largely deviates from lognormal distribution. The results obtained from WA and SYA respectively can be compared to tell how well the distribution of the sum fits lognormal. The smaller the difference, the better the fit. This is because the two methods derive their results independently while their results are only connected by the mapping of lognormal. When σ is fixed and small for all variables, the distribution of the sum highly resembles lognormal and both methods work well. Fig. 1 shows u_α and σ_α for varied J in MRC and EGC cases. The curves obtained by different methods overlap totally indicating complete agreement. The parameters involved in plotting the graph are given in section IV.

[1]Note that there are some different definitions of lognormal distribution and a scaling should be applied during transformations between them.

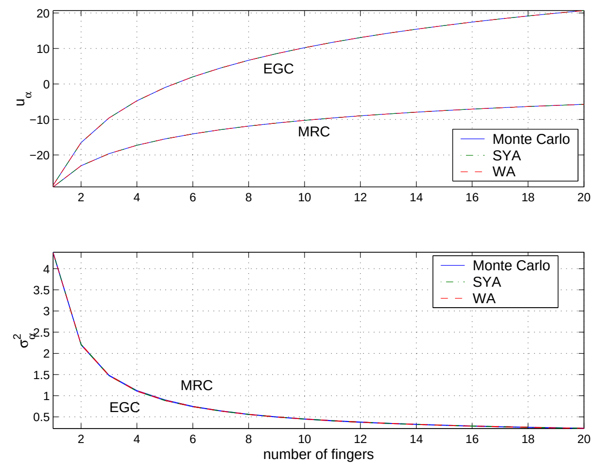

Fig. 1. The u_α and σ_α^2 for MRC and EGC obtained by the methods of Monte Carlo, SYA and WA where $\varepsilon_0 = 0.035$, $\sigma = 3.3941$dB and Γ=4.3. The curves obtained by 3 methods overlap each other.

B. Derivation of Explicit Expressions of Performance

With the known distribution of the random factor in the instantaneous SNR, α, performance of RAKE can be readily evaluated.

The mean and variance of i-SNR can be obtained by

$$\text{E}[\gamma_s] = \lambda \text{E}[\alpha], \tag{11}$$

$$\text{Var}[\gamma_s] = \lambda^2 \text{Var}[\alpha] = \lambda^2 \big(\text{E}[\alpha^2] - (\text{E}[\alpha])^2\big). \tag{12}$$

The SEP conditional on α is given by

$$\Pr(e|\alpha) = Q(\sqrt{\gamma_s}) = \frac{1}{\sqrt{2\pi}} \int_{\sqrt{\gamma_s}}^{+\infty} \exp(-y^2/2) dy. \tag{13}$$

Averaging the $Pr(e|\alpha)$ over α, we obtain the mean SEP as

$$\Pr(e) = \text{E}_\alpha[Pr(e|\alpha)] = \int_0^\infty Q(\sqrt{\gamma_s}) p(\alpha) d\alpha, \tag{14}$$

where $p(\alpha)$ is the pdf of α.

The mean SEP can be evaluated numerically via Monte Carlo simulation with (14). An alternative way can be used to arrive at an explicit expression, considered next.

Let $\beta = (20\log_{10}\alpha - u_\alpha)/(\sqrt{2}\sigma_\alpha)$ and exchange α in (14) with β, yielding

$$\Pr(e) = \frac{1}{\sqrt{\pi}} \int_{-\infty}^{\infty} Q\Big(\sqrt{\lambda 10^{(\sqrt{2}\sigma_\alpha\beta + u_\alpha)/20}}\Big) \exp(-\beta^2) d\beta. \tag{15}$$

In consideration of the weight function $\exp(-\beta^2)$, (15) can be best computed numerically by Hermite-Gauss Quadrature [12],

$$\Pr(e) \simeq \frac{1}{\sqrt{\pi}} \sum_{n=1}^{N_h} H_{x_n} Q\Big(\sqrt{\lambda 10^{(\sqrt{2}\sigma_\alpha x_n + u_\alpha)/20}}\Big), \tag{16}$$

where N_h is the order of the Hermite polynomial $H_{N_h}(\cdot)$, x_n and H_{x_n} are the zeros (abscissas) and weight factors of N_h-order Hermite polynomial, respectively. These values are tabulated in many mathematical handbooks (e.g., [12]). In section IV, we show $N_h = 16$ can generate very accurate results where only 16 coefficients are required in the computation.

IV. Numerical Examples

For binary PPM, in the case of optimal modulation, ρ is generally in the range of $(0.5, 1)$ depending on the pulse used. For bipolar modulation, ρ equals to 1. For convenience, bipolar modulation is adopted to exemplify the effects of RAKE reception below.

For single exponential decay model, parameters are chosen as below:

- Set $\varepsilon_0 = 1/(4\pi d^2)$ to account for free space propagation where d is the distance between the transmitter and receiver;
- Instead of simulating a poisson process, interval of multipath arrival is modelled as fixed. Set $\tau_\ell = 0.167(\ell - 1)$ns to demonstrate a system in which central-frequency equals 6GHz and multipath-delay interval equals 0.167ns;
- $\Gamma = 4.3$ and $\sigma = 3.3941$dB corresponds to the ray decay factor and standard deviation of ray lognormal fading term of CM1 in [2], respectively;

For the dual exponential fading model in [2], we use the data of average power profile of CM1 generated by the program in [2]. The first arrived path is excluded due to the large deviation between it and the succeeding paths.

Figs.2-5 demonstrate the performance based on single exponential decay channel. All figures show EGC has comparable performance with MRC. This alleviates the channel estimation problem greatly.

Fig. 2 shows how the mean and variance of i-SNR vary with J, Fig. 3 demonstrates the variation of mean SEP with J for fixed transmitted SNR E_s/σ_0^2, and Fig. 4 depicts how the mean SEP varies with E_s/σ_0^2. The numerical computation of mean SEP is based on (16) with $N_h = 16$. It is clear that Hermite-Gauss quadrature generates very accurate results. Comparing Fig. 3 and Fig. 4, we can find that increasing the transmitted SNR E_s/σ_0^2 have much better improvement on the SEP compared to increasing the number of RAKE fingers J.

In addition, some experiments on the parameters of the channel model indicate that 1) performance slightly changes and performance difference between MRC and EGC slightly increases with σ increasing; 2) with Γ increasing, performance is improved slowly since the mean power of paths decays more slowly and more power can be collected; 3)with ε_0 increasing, the mean SEP decreases rapidly. Fig. 5 shows how the SEP changes with the distance d between transmitter and receiver.

The mean SEP based on the dual exponential fading model in [2] is displayed in Fig.6 to show the relationship between MRC and EGC in three situations. The lines without marks correspond to the theoretical result when applying the average power profile of CM1 in our analysis method. For comparison, the marked lines represent the statistical results directly from

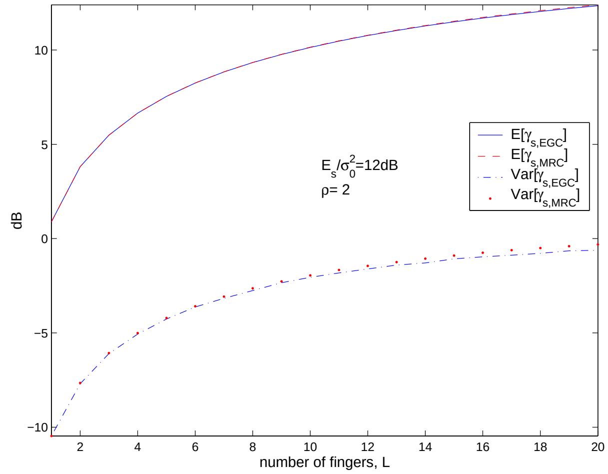

Fig. 2. The mean and variance of i-SNR versus the number of RAKE fingers J in EGC and MRC cases when $E_s/\sigma_0^2 = 12$dB, $d = 1.5$m.

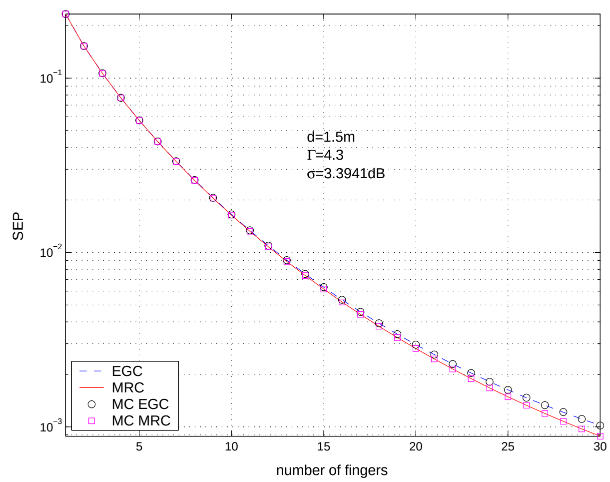

Fig. 3. The mean SEP obtained by (16) and Monte Carlo simulation (MC) versus the number of fingers J in EGC and MRC cases when $E_s/\sigma_0^2 = 12$dB, $d = 1.5$m.

the experimental data generated from CM1. Between them, the line marked with circles is based on the original continuous model and the other marked with triangles is based on the sampled discrete model in which the nonzero fingers are chosen. The transmitted SNR here is different for the three cases and is not given due to the unknown gain of the channel models. From Fig.6, we can see that EGC still has comparable performance with MRC in the first two situations, while the difference between them is enlarged in the discrete model. The possible reason is that the discretization of the continuous model causes combination/sum of adjacent paths which have time duration smaller than the sampling time. During each realization, the sum could happen among paths with opposite or same polarity. Then large difference could be arisen among different realizations which makes it possible that the average power profile could not correctly reflect the statistical property of the channel. This is also the cause of large fluctuation of average power profile. This implies there are limitations of our

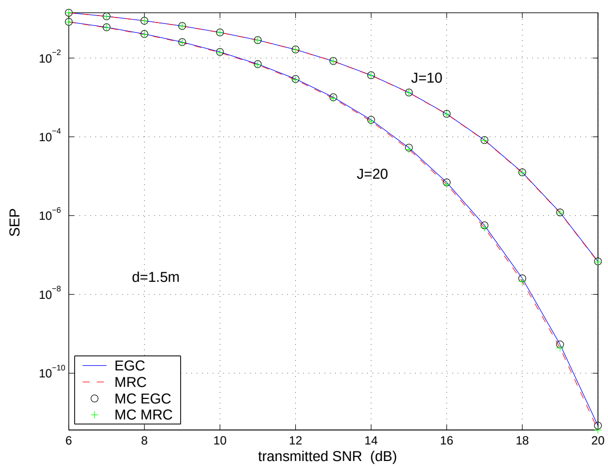

Fig. 4. The mean SEP obtained by (16) and Monte Carlo simulation (MC) versus transmitted SNR E_s/σ_0^2 in EGC and MRC cases when $d = 1.5$m, $J = 10$ and 20.

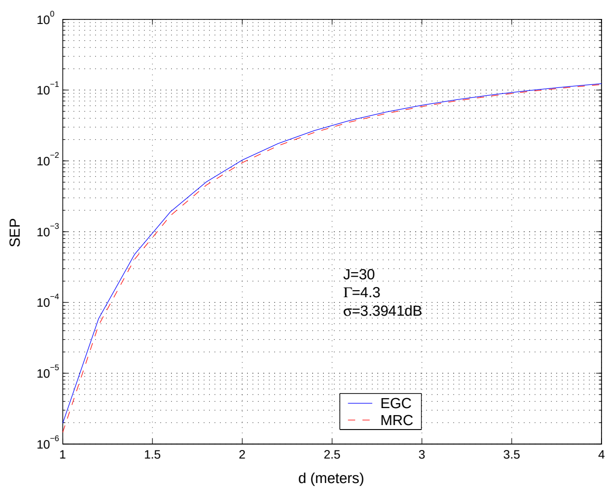

Fig. 5. The mean SEP obtained by (16) versus d in EGC and MRC cases when $E_s/\sigma_0^2 = 12$dB, $J = 30$.

model on modelling sampled channels.

V. Conclusions

The performance of RAKE reception for UWB is evaluated in a lognormal-fading channel. Firstly, we address that in most cases, both the property of TH codes and modulation methods determine whether ICI can be mitigated to a negligible degree. It is emphasized that without further design, the orthogonal PPM is not applicable to TH-UWB in the sense of possibly detrimental ICI. With the “clean” output, a simple way is suggested to derive explicit performance expressions for various combining methods based on the fact that the sum of lognormal variables can be well approximated by another lognormal variable under appropriate conditions. Numerical results indicate that RAKE reception can is very effective for UWB, and equal gain combining has comparable performance with maximal ratio combining.

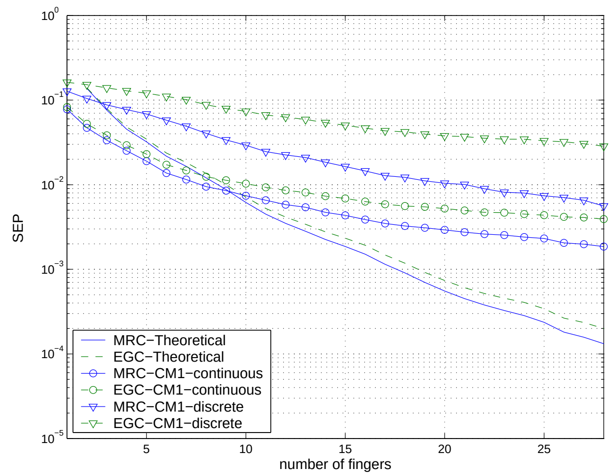

Fig. 6. The mean SEP in EGC and MRC cases when $\sigma = 6.4$dB, a) theoretical results; b)statistical results based on continuous model in [2]; c) statistical results based on discrete model in [2].

References

[1] D. Cassioli, M. Z. Win, F. Vatalaro, and A. F. Molisch, “Performance of low-complexity Rake reception in a realistic UWB channel,” *IEEE International Conf. on Communications (ICC)*, vol. 2, pp. 763–767, 2002.

[2] J. Foerster et al., “Channel modeling sub-committee report final,” *IEEE P802.15 Working Group for Wireless Personal Area Networks (WPANs), IEEE P802.15-02/490r1-SG3a*, Feb. 2003.

[3] T. Erseghe, “Time-hopping patterns derived from permutation sequences for Ultra- Wideband impulse-radio applications,” *6th WSEAS International Conference on Communications, Crete*, vol. 1, pp. 109–115, July 7-14 2002.

[4] R. A. Scholtz, P. V. Kumar, and C. J. Corrada-Bravo, “Signal design for Ultra-wideband radio,” *Sequences and Their Applications (SETA ’01)*, May 2001.

[5] R. Price and P. E. Green, “A communication technique for multipath channels,” *Proceedings of The IRE*, vol. 46, pp. 555–570, Mar. 1958.

[6] F. Ramłrez-Mireles, “On the performance of Ultra-Wide-band signals in Gaussian noise and dense multipath,” *IEEE Trans. Veh. Technol.*, vol. 50(1), pp. 244–230, Jan. 2001.

[7] J. Zhang, R. A. Kennedy, and T. D. Abhayapala, “New results on the capacity of M-ary PPM Ultra Wideband systems,” *IEEE International Conf. on Communications (ICC)*, May 2003.

[8] M. S. Alouini and A. J. Goldsmith, “A unified approach for calculating error rates of linearly modulated signals over generalized fading channels,” *IEEE Trans. Commun.*, vol. 47(9), pp. 1324–1334, Sep. 1999.

[9] L. F. Fenton, “The sum of log-normal probability distributins in scatter transmission systems,” *IRE Trans. on Communications Systems*, vol. CS-8, pp. 57–67, Mar. 1960.

[10] S. C. Schwartz and Y. S. Yeh, “On the distribution function and moments of power sums with log-normal components,” *The Bell System Technical Journal*, vol. 61(7), pp. 1441–1462, Sep. 1982.

[11] C. L. Ho, “Calculating the mean and variance of power sums with two log-normal components,” *IEEE Trans. Veh. Technol.*, vol. 44(4), pp. 756–762, Nov. 1995.

[12] A. H. Stroud and D. Secrest, *Gaussian Quadrature Formulas*, Prentice-Hall, Inc., Englewood Cliffs, N.J., 1966.